# Effects of Remaining Hair Cells on Cochlear Implant Function

4th Quarterly Progress Report

Neural Prosthesis Program
Contract N01-DC-2-1005
*(Quarter spanning April - June, 2003)*

P.J. Abbas, C.A. Miller, B.K. Robinson, F.C. Jeng, K.V. Nourski,

Department of Otolaryngology-Head and Neck Surgery
&
Department of Speech Pathology and Audiology

University of Iowa

Iowa City, Iowa, USA

July 31, 2003

File: N01-DC-2-1005QPR04.PDF

Effects of Remaining Hair Cells on Cochlear Implant Function
N01-DC-2-1005QPR04
Neural Prosthesis Program

## Table of contents

# 1. Introduction

The goal of this contract work is to investigate how the presence of viable hair cells may influence the auditory nerve's response to intracochlear electrical stimulation. In this fourth quarterly progress report (QPR #4), we continue our investigation of single auditory nerve fiber recordings in two directions:

First, we extend the study first described in QPR #2, which examined the effect of wideband acoustic noise on fiber responses to single electric pulses. This analysis provides a description of how added acoustic noise influences basic electric response properties of firing rate, relative spread and jitter.

Second, as the focus of this report, we extend the study described in QPR #3 which examined how the electrically evoked compound action potential (ECAP) produced by a train of electric pulses is modified by the presentation of wideband acoustic noise. We present analogous measures obtained from single fibers to provide a more complete picture of the response properties underlying the trends reported in the ECAP data.

# 2. Summary of activities in this quarter

During the fourth quarter of this contract (April 1 through June 30, 2003), we accomplished the following:

1. Prepared and submitted a short communication to Hearing Research on ototoxic interaction of kanamycin and ethacrynic acid in acute experimental preparations (discussed in the second QPR).

2. Attended and presented findings at the Third International Symposium on Objective Measures in Cochlear Implants at Ann Arbor, Michigan.

3. Revised the peer-reviewed manuscript submitted to Hearing Research (Hu *et al.*, 2003) that details the experiments and findings described in QPR #1.

4. Completed analyses of single-fiber data examining the responses to single electric pulses imbedded in acoustic noise. Those data are summarized in Section 3 below.

5. Data from acute experiments measuring the ECAP in guinea pig preparations were presented in the last QPR. That work examined the combined effects of electric pulse train stimuli and wideband acoustic noise presented simultaneously. Three additional experiments were conducted examining the responses with longer duration stimuli to further assess effects of adaptation and recovery. Results are being analyzed and will be presented in the next QPR.

6. We performed three acute experiments on cats to measure single-fiber responses to combinations of electric and pulse train stimulation. Initial results are summarized in Section 4 below.

## 3. Effects of acoustic noise on single-fiber responses to single electric pulses

In QPR #2, we presented initial progress in the examination of the effect of simultaneously presented wide-band acoustic noise on single-fiber responses to single-pulse electric stimuli. One working hypothesis of acoustic-electric interaction suggests that ongoing single-fiber activity elicited by acoustic stimulation will alter the response characteristics of the fiber when simultaneously stimulated with an electric current pulse. One possible cause of interactions could be the acoustically induced state of partial refractoriness. Our previous work (Miller et al., 2001) has shown that the state of partial refractoriness can alter relative spread (Verveen, 1961), i.e., the fiber's dynamic range to the electric stimulus.

In this report, we present some additional data from another acute cat preparation (D01) that has now been analyzed. This additional data set confirms, but does not fundamentally alter, the trends reported in QPR #2.

### 3.1 Methods

The methodology used to collect these data is similar to that used in previous experiments. Acute experimental sessions were performed on healthy, adult, cats, free from signs of middle-ear infection. General surgical techniques have been described in Miller et al. (1999). Briefly, the cat was anesthetized with Nembutal and the auditory nerve was surgically exposed. The left bulla was opened using a surgical drill to reveal the basal aspect of the cochlea. Click-evoked compound action potentials were obtained both before and after drilling a small cochleostomy into the basal turn of scala tympani (using a 0.5 mm diamond burr). A stimulating electrode was then inserted into this defect. This electrode was fashioned by flame-balling a Teflon-coated 0.003" diameter Pt/Ir wire to a diameter of approximately 0.35 –0.45 mm. This electrode was inserted into the defect to a depth between 0.5 and 1.0 mm. In the case of the subject reported here (subject D01), the post-insertion CAP measures indicated an upward threshold shift of 15 dB, due, presumably, to insertion trauma.

The electric stimulus consisted of a single rectangular (40 us/phase) biphasic current pulse delivered to the monopolar intracochlear electrode. A needle electrode inserted into a forepaw served as the return current path. The interpulse interval was 30 ms and the polarity of each successive pulse was alternated. The acoustic stimulus was generated by a Grason Stadler noise generator, with the level controlled by an attenuator. This stimulus was transduced by a Beyer DT-48 earphone mated to the external meatus by a otoscopic speculum. This mating was improved by means of a silk ligature tied around the portion of the meatus that overlapped the speculum. For this experiment, sound pressures were monitored by a probe microphone mounted within the speculum (note: monitoring procedures have subsequently been modified, as described in Section 5, below).

Prior to single-fiber data collection, the electrically evoked compound action potential was recorded at several (3-8) levels so as to obtain an input-output function and an estimate of the nerve's dynamic range to the electric stimulus. While searching for units, only the electric stimulus was presented, using a level that evoked an ECAP amplitude of 80-90% that of the saturation (maximum) response amplitude. Once a fiber was encountered, a series of responses were recorded at levels spanning the dynamic range of the fiber. For each level, responses to 100 repeated stimuli were recorded. After the electric-only response was characterized, the acoustic noise was presented at a relatively high level (98 dB SPL overall level) to maximize the probability of an acoustic response. The noise was turned on for at least 30 s prior to collecting responses to both the noise and electric pulse stimuli (repeating the electric levels used in the initial, no-noise, condition)

Single-fiber potentials were recorded using a glass micropipette electrode and an Axoprobe (Axon Instruments) headstage and amplifier. Potentials were low-pass filtered by this device (10 kHz cutoff, 2-pole filter) and high-pass filtered at 100 Hz by a custom-built two-pole Butterworth filter. These filtered potentials were then digitally sampled at a rate of 100,000 sample/s with a 16-bit Data Translation ADC board controlled by custom (in-lab) software. All waveforms were stored to files for detailed analysis conducted after the conclusion of the experiment. These analyses were conducted using custom software written using Matlab routines (version 6).

The main goal of this experiment was to assess alterations to the electric response induced by the simultaneous presentation of acoustic noise. Thus, we sought to analyze the electric response to direct membrane depolarization and used a post-stimulus time analysis window of 1 ms to eliminate any long-latency responses that could be attributed to electrophonic activity. For each fiber, we also recorded the fiber's response to the acoustic noise presented alone for a total recording period of 800 milliseconds. This estimate allowed us to perform a correction to the electric input-output functions (Sachs & Abbas, 1974) so that those functions could provide a better estimate of the electric response. In almost all cases, this correction resulted in negligible (<5%) changes in our estimates of threshold and relative spread.

### 3.2 Results

Sixteen fibers were contacted for a sufficient time to collect input-output functions to both the electric-only and electric+acoustic stimulus conditions. As was done in QPR #2, the fiber responses were analyzed for threshold (defined by the electric level producing a firing efficiency of 50%), jitter (the standard deviation of spike times recorded in the 1 ms analysis window) and relative spread (expressed in %).

Figure 1 plots these three measures as a function of the spike rate to the acoustic stimulus presented alone. Data from both subject D01 and C93 (i.e., the data presented in QPR #2) are shown in the graphs. As was done before, we have computed the linear regression fits to each fiber's threshold, jitter, and RS plots to determine overall trends (applying linear regression over the combined, group, data would be inappropriate due to across-fiber differences in driven spike rates). As was the case for C93, a majority of the fibers from subject D01 demonstrated positive correlations of each of the three measures with increases in the acoustically driven spike rates. We computed the mean changes in each of these measures for a change in the acoustically driven rate from 0 to 100 spike/s. For that change, the mean change in electric threshold was approximately 3 dB and the mean change in jitter was about 0.1 ms. The mean change in relative spread was about 5%, that is, relative spread approximately doubled its value.

Although these changes are rather modest, they do suggest that the simultaneous presence of acoustically driven activity may be advantageous for the encoding of electric stimuli. It is clear, however, that these results require follow-up research using more complex electric stimuli.

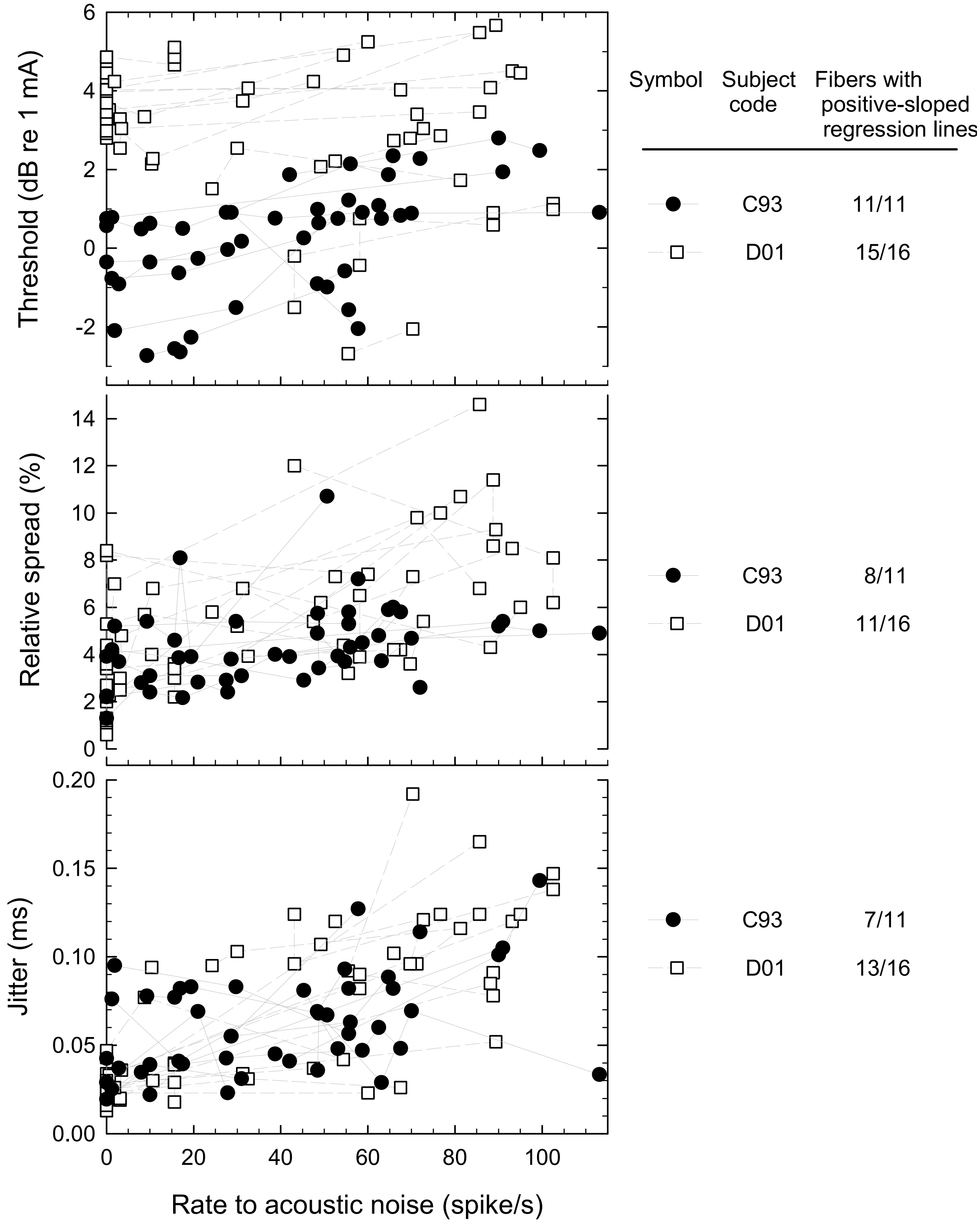


**Figure 1** Summary of single-fiber data from two cats showing the effect of acoustically driven spike activity on three measures of the spike activity elicited in response to a single, 40 us/phase biphasic, electric pulses. The fractions shown along the rightmost column indicate the number of fibers that demonstrated a positive correlation between the two plotted variables, as assessed by linear regression.

# 4. Effects of Acoustic noise on single-fiber responses to electric pulse trains

## 4.1. Introduction

Our work using the ECAP in the initial contract period demonstrated interactions between acoustic and electric stimulation (Abbas et al., 2002). When presented simultaneously, noise has the effect of decreasing the amplitude of ECAP response. Based on our single-fiber data (this report and Miller et al., 2001), we believe that this may be due to a combination of effects, including increased threshold, decreased synchrony, and reduced action-potential amplitude. We also suspect that a combination of refractory and adaptation-like responses may be relevant. For the analysis of ECAP responses presented in QPR #3, we employed an acoustic noise burst imbedded in an electric pulse train in order to assess the time course of this acoustic-electric interaction. Results from those experiments demonstrated that noise produced a decrease in the ECAP amplitude to the pulse train and the time course of that effect was consistent with the expected pattern of discharge rate to the noise over time. The effect of the noise was greatest at the time of its onset and that effect decreased to an approximate steady state within 50 ms. These effects were largest for relatively long electric interpulse intervals (4 ms vs 1 ms) and for higher levels of the acoustic noise. In addition to the simultaneous effects of noise, we also observed effects on the ECAP to the pulse train just after the noise offset, presumably due to some residual effect. In most cases, this effect of the noise was a depressed response to the electrical stimulus. In a few subjects, we observed a more complex recovery pattern which could include a period of enhanced response amplitude. Finally, we noted in our initial single-fiber study (see QPR #2, Figure 4) trends suggesting that residual effects of the acoustic stimulus on the electric response can be observed after cessation of the acoustic stimulus.

As we have noted before, a straightforward hypothesis relative to the effect of noise on the electric response may be that neural activity in response to the noise may reduce or desynchronize the responses to the electric pulse train. The time course of observed ECAP decrements shortly after noise onset is consistent with this hypothesis in that there is initially a large effect of the noise followed by an approximately exponential recovery. The expected activity in response to the noise would show a similar time course. The overshoot, or increased response, that we have observed after noise offset in some cases is also consistent with this hypothesis. However, the residual masking effect observed, in many cases, the response observed after noise offset is not consistent with that simple hypothesis. This post-noise effect suggests that adaptation caused by an acoustic stimulus can influence later, subsequent, neural responses to electrical stimuli.

The complex pattern of recovery observed in the ECAP findings suggests that there may be multiple mechanisms involved in the masking effects. Detailed descriptions of auditory nerve fiber response properties such as spike rate, jitter, and synchronization index would be helpful in providing a better understanding of the observed influence of acoustic noise. Experiments described in this section examine single-fiber responses using an acoustic-noise / electric-train stimulus paradigm similar to that used in our previously reported ECAP experiments.

## 4.2. Methods

Animal preparation, stimulus apparatus, and recording methods have been described in Section 3. However, acoustic calibration procedures were modified as described I Section 5 and we developed new data collection routines. Stimulus generation and recording were accomplished using an Instrutech ITC-18 interface controlled through a Labview program running on a PC. Stimuli used are illustrated in Figure 2. These initial experiments were conducted using electric pulse trains composed of 40 us/phase

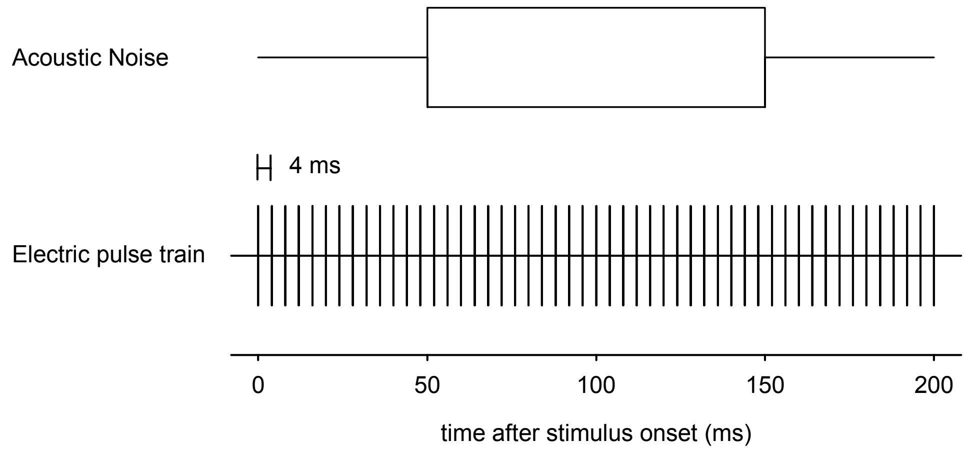


biphasic pulses presented at an interpulse interval (IPI) of 4 ms. This rate was chosen as our ECAP data

**Figure 2** Schematic representation of the acoustic noise burst (top) and electric pulse train (bottom) used in the single-fiber studies described in Section 4. Presentations of the pulse train with the noise are interleaved with presentations of the train without the noise to afford comparisons between the two conditions.

demonstrated significant effects of noise at a 4 ms IPI. The duration of the pulse train was 200 ms and the noise was gated on at 50 ms after pulse train onset and gated off at 150 ms. While this duration was somewhat shorter than that used in ECAP experiments, we chose the shorter duration to reduce data collection time with the hope of collecting data for more stimulus conditions per fiber. The "off" time between each pulse-train presentation was 800 ms. Sampling rate for both stimulus output and data input was 100,000 sample/s. Stimuli with electric pulse train alone were alternated with stimuli with electric pulse train plus acoustic noise. In that way comparisons could be made of the neural responses to the electric pulse train both with and without the added acoustic stimulus. For each stimulus condition, we recorded responses to 50 repeated presentations in order to estimate firing statistics and construct post-stimulus-time histograms.

All response traces were saved and analysis was conducted off-line. Removal of stimulus artifact was accomplished using a modification of the technique described in Miller et al. (1999). A "stimulus artifact template" was calculated for each pulse in the train by averaging response traces where there were no action potentials in response to that pulse using the electric pulse train alone. The templates were calculated over each 4 ms (IPI) interval and the sequence of templates could then be subtracted from the entire response to the pulse train for both the pulse train alone and pulse train + noise conditions. This method could reliably subtract out both the stimulus artifact and ECAP response that was evident in the raw data. After the artifact was subtracted, a criterion level was chosen to identify action potentials and both the peak amplitudes and latency of action potentials were determined. Both dot raster plots and histograms were then saved for plotting and further analysis. The histogram bin width was set at 100 us, i.e., ten sampling periods.

### 4.3. Results

Significant data (>20 fibers) have been collected from three subjects. The results of the first subject (subject D10) have been analyzed and make up the majority of the data reported here. Based on the results from this subject, we have made some changes in the experimental paradigms in order to pursue the trends observed in the initial experiment. These changes are discussed in the following section, below. In the first experimental animal, we chose the level of noise to be relatively high (in most cases 97 SPL) in order to maximize the effects of noise on the electric response. The electric current levels were varied across the dynamic range of the fiber. In the fiber data shown in this report, most of the levels chosen were within the lower part of the fibers' dynamic ranges (i.e., 20%<FE<90%) as indicated by the histogram data for the first pulse.

Results from two typical fibers are shown in Figure 3. The analysis presented in this and the following two figures share a common format. The graphs of the top two rows show the histograms recorded for the two major stimulus conditions (electric train alone and electric train + noise conditions). The lower three rows of graphs provide analyses of (1) the number of spikes, (2) vector strength, and (3) jitter, calculated for each 4-ms long interval following each electric pulse. In Figure 3, the pulse-train alone condition (labeled "electric") shows a series of peaks that are highly synchronized to the 4-ms IPI pulse train stimulus. The histograms in response to pulse train and the noise stimulus ("electric+acoustic") show a period of highly asynchronous activity, presumably in response to the noise burst gated on at 50 ms and off at 150 ms. The pattern of the histograms obtained after the time of noise are similar for both the "electric" and "electric+acoustic" conditions, again showing high synchrony to the electric pulse train.

The additional analyses shown in the graphs of the lower three rows provide an assessment of the time course of changes in discharge rate, vector strength, and spike jitter. For all three measures, the response patterns over the first 50 ms are similar for both the "electric" and "electric+acoustic" conditions, as would be expected. The "electric+acoustic" condition shows a sharp increase in spike rate at 50 ms with the onset of the noise and a gradual asymptote to an approximate steady state. After stimulus offset, the response to the pulse train in the two conditions are similar, i.e., there is no apparent residual effect on the discharge rate.

We evaluated the synchronization of responses with two measures, vector strength and jitter. The vector strength for each 4 ms period is shown in the graphs of the fourth row of Figure 3 and the jitter measures are plotted in the lowest row. We note that the jitter calculation in these cases is somewhat different than that used in our single-pulse measures (such as those of Figure 1). In that data, the response window was relatively narrow (1 ms) while in this case jitter calculations were based on the 4 ms window over which other assessments were made. Both vector strength and jitter show clear changes with the presentation of the noise indicating, as is clear from the histogram, that synchronization is reduced. While there tends to be clear onset effect in rate, vector strength and jitter do not show comparably clear changes over the period of noise presentation.

Figure 4 presents data from two additional fibers that demonstrated similar response patterns. Specifically, there was a clear increase in response to the noise, an increase in spike count at noise onset decreasing to a steady state and an approximately constant effect on vector strength and jitter over the 100-ms noise burst. In the data of these two fibers, however, we noted evidence of a residual effect of noise after the noise offset. The "electric+acoustic" histograms of both fibers exhibit slight reductions in the peaks that occur in the 10-20 ms after noise offset. Those reductions are also reflected in the spike counts in the intervals from 150 to 180 ms in the third row of graphs (spikes per period). No apparent residual effect is evident in the vector strength or jitter.

Figure 5 shows examples of data from a fiber demonstrating differences in the response to two levels of electric current. The data shown in the left column was obtained at a level where the response to a single pulse was at maximum FE. The right column shows data from the same fiber for a stimulus level in the

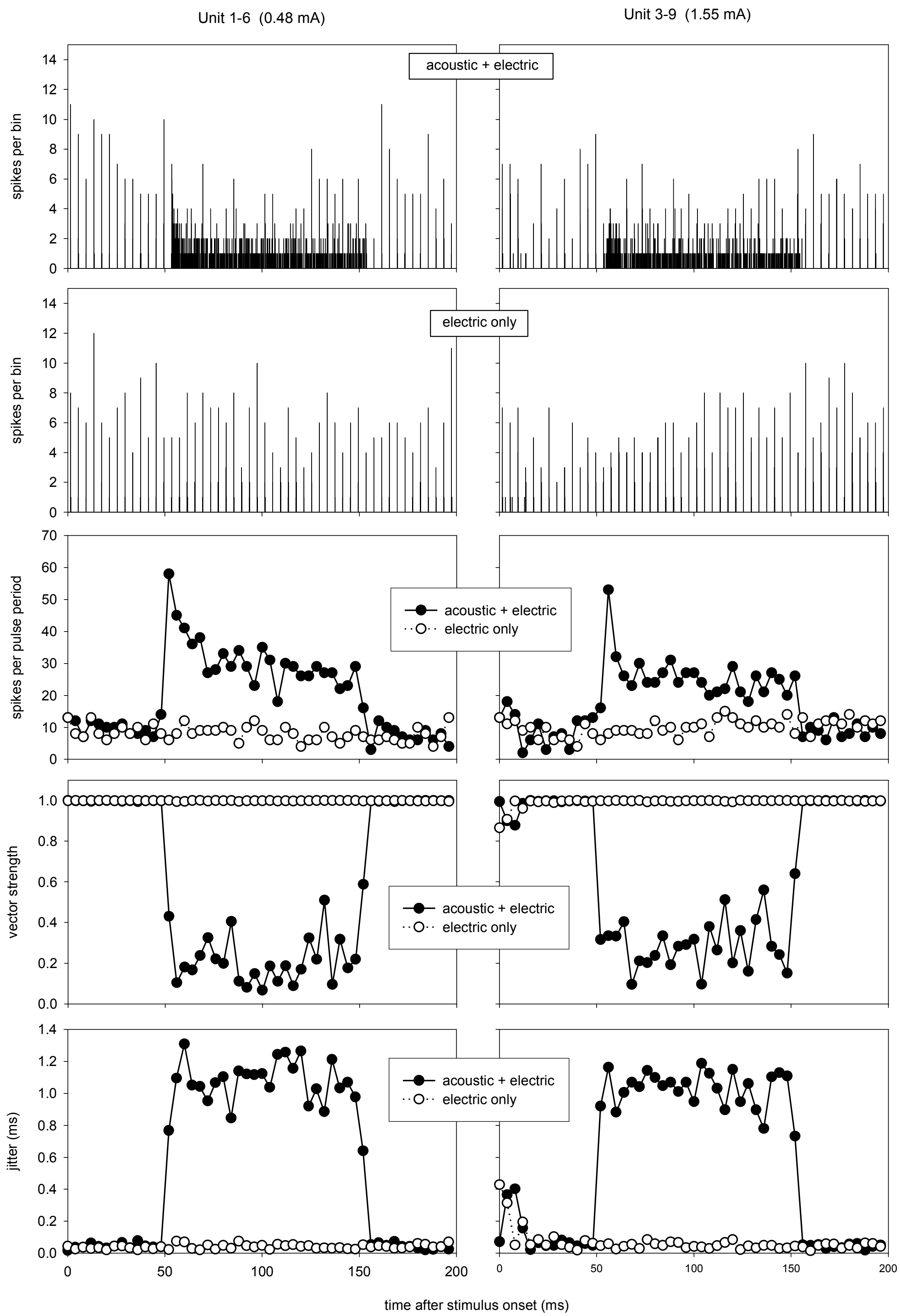


**Figure 3** Analysis of single-fiber responses to combinations of acoustic noise and electric pulses. Data for two fibers are shown here, with current level indicated at the top. The noise level was 97 dB SPL (overall level). The first row of graphs plots PST histograms across the pulse-train duration; the noise was gated on and off at 50 and 150 ms, respectively. The second row plots histograms for the electric train alone. The third through fifth rows plot analyses of spike patterns (spike counts, vector strength, and jitter) in each 4-ms time window corresponding to the period of the pulse train.

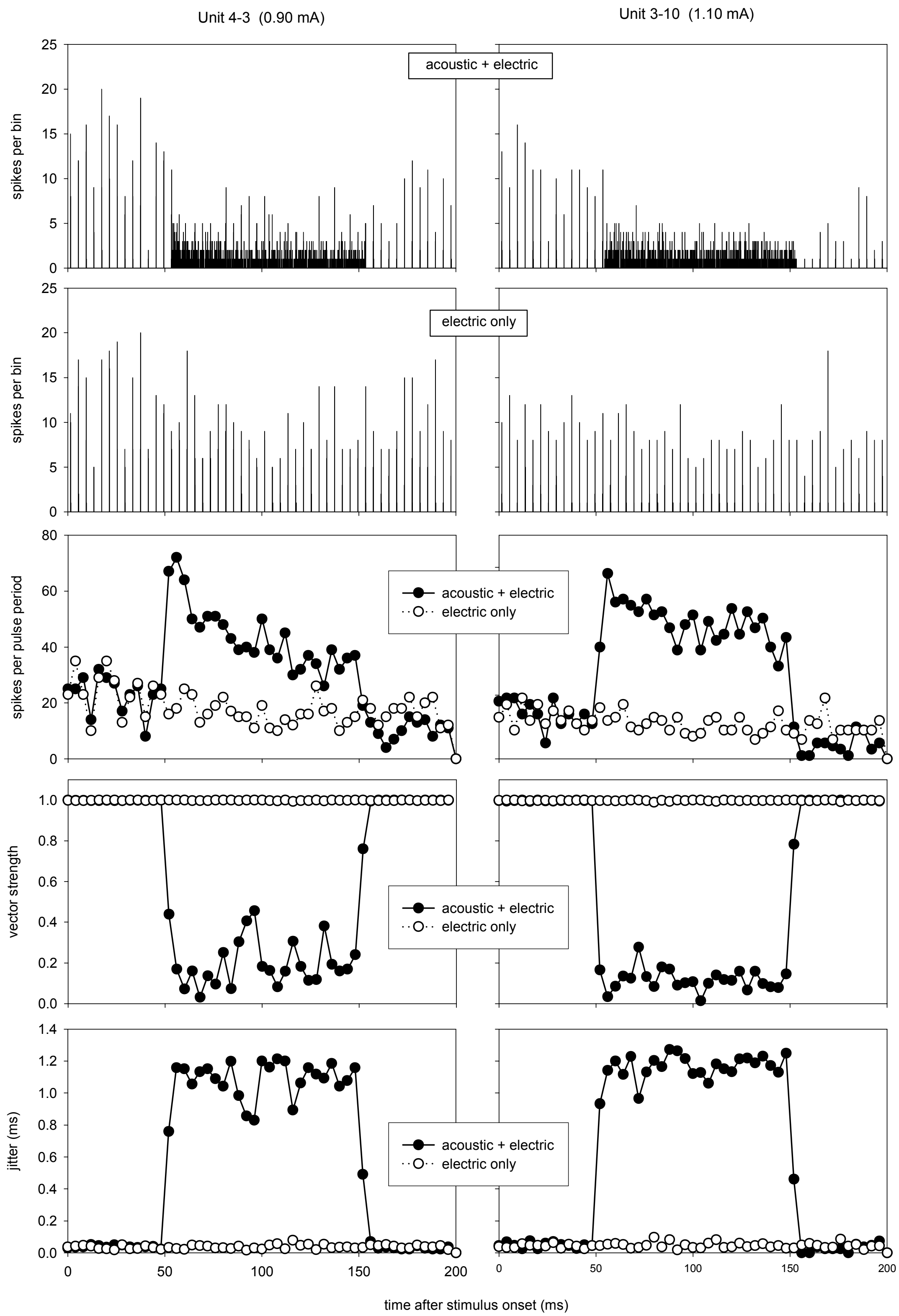


**Figure 4** Single-fiber response analysis for two additional fibers, using the same methods and format as was used in Figure 3. Current levels were held constant at the values indicated at the top; the noise level was 97 dB SPL (overall level). These data demonstrate a residual effect on spike count (graphs of row 3) that occurred after the offset of the acoustic noise.

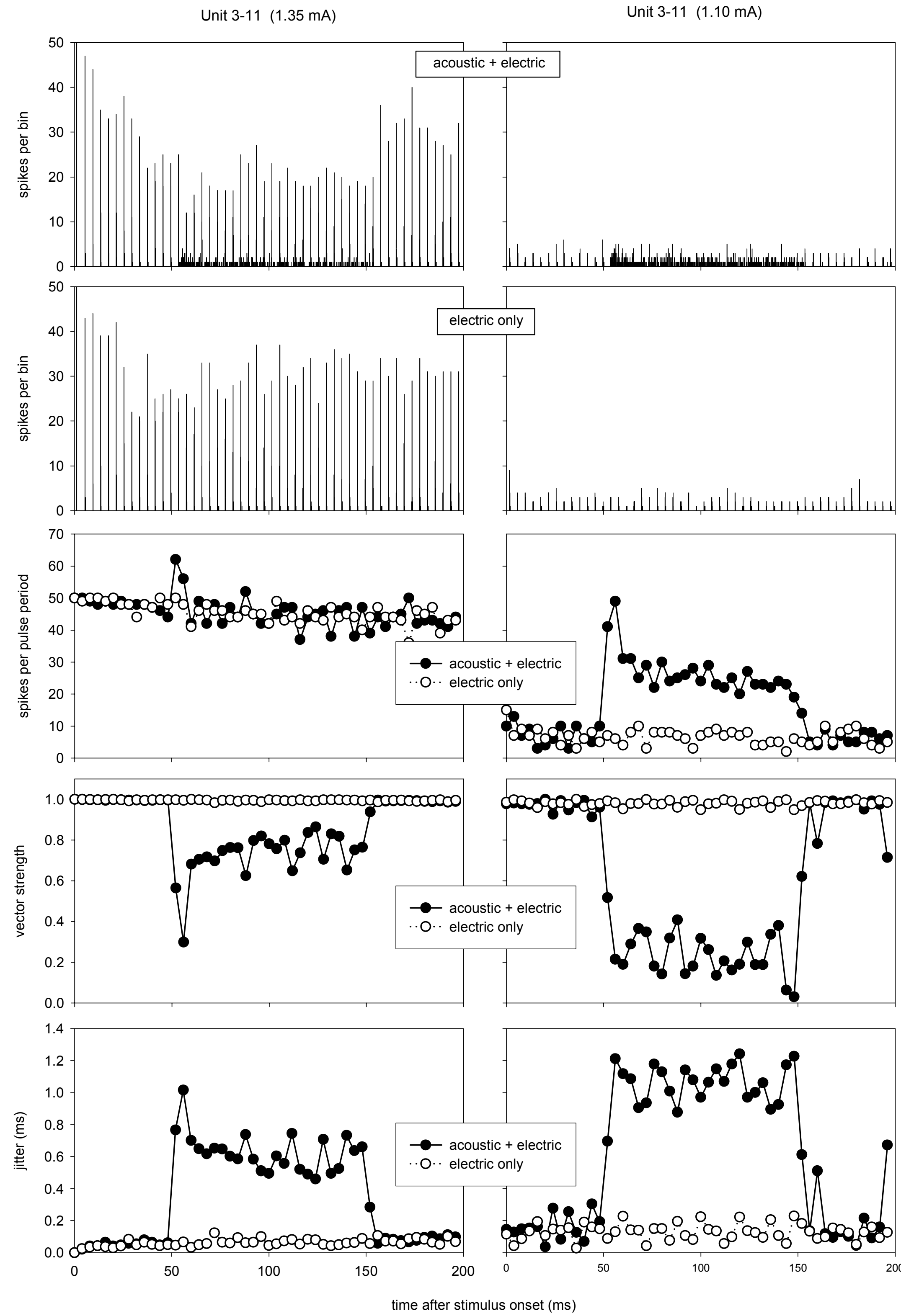


**Figure 5** Same analysis of patterns of action potentials as in Figure 3. In this case, data are shown for a single fiber studied at two different electric levels (see top of columns). Noise level is again fixed at 97 dB OAL.

lower part of the dynamic range (as assessed by the first-pulse response). The response patterns are quite different across the two levels. At the lower current level (right column) there is little synchrony in the acoustic + electric condition. At the higher level (left column), with the same level of noise, the synchrony to the pulses is affected, but still shows clear peaks in the histogram. Unlike the data for the lower electric level, the spike counts show a slight elevation at onset for the high level stimulus but show no change over most of the noise burst. Despite the similar discharge rates during the noise, vector strength and jitter are both clearly affected, with the response to the lower-level electric stimuli affected to greater degree. Both vector strength and jitter also show a higher effect at noise onset that is not evident at the higher stimulus level (data plotted in left column). These data demonstrate the importance of evaluation of these effects over a range of stimulus levels.

We also performed histogram data reduction in order to examine trends across a group of fibers. Subject D10 provided us with data sets from a total of 19 fibers that were responsive to both acoustic and electric stimulation. In this analysis, we computed two response statistics, (1) total number of spikes and (2) vector strength over five analysis windows spread across the duration of the stimulus. Each of these analysis windows was 20 ms in duration and is described in the following table.

| *Window* | *Duration (ms)* | *Description of analysis time window* |
|---|---|---|
| 1 | 1-21 | Beginning just after the onset of the electric pulse train |
| 2 | 29-49 | Ending just before onset of the acoustic noise stimulus |
| 3 | 55-75 | Beginning after the onset of the acoustic noise burst |
| 4 | 129-149 | Ending just before the offset of the noise burst |
| 5 | 155-175 | Beginning just after the offset of the noise burst. |

To characterize responses across this group of fibers, we chose a current level at which the firing efficiency (to the first pulse) was between 20 and 80%, i.e., within the fiber's dynamic range. To make this group analysis tractable, we also reduced the data by normalizing the measures obtained under the "electric+acoustic" to those obtained under the "electric" alone condition. Thus, total spike count, for example, is expressed as the spike count obtained in the "electric+acoustic" condition divided by the count obtained with the "electric" only stimulus condition. The data are plotted in Figure 6 as a function of the number of each analysis window. Before onset of the noise (i.e., windows 1 and 2) the values are approximately one, as expected. During presentation of the noise (windows 3 and 4) there is a clear increase in discharge rate and a clear decrease in vector strength. After noise offset, there is a slight decrease in the spike count in some fibers. However, this residual effect failed to achieve statistical significance across the population (i.e., the mean value is not significantly different than one).

Similar analyses are shown in Figure 7 for one fiber in which we have analyzed the data from several levels of electric pulse train as well as several levels of noise. In the upper row of graphs, data are shown for four current levels with a constant level of noise (97 dB SPL). In the bottom row of graphs, the current level is held constant (1.15 mA) and the level of noise is varied. The effect of noise on both the spike counts and vector strength is greatest for higher levels of noise and for lower levels of pulse train, that is, when the noise level to current level ratio is larger. In addition, the residual effect of noise (analysis window 5) tends to be greater under those same conditions. These data suggest that at under certain stimulus conditions, the residual effects of noise may be more prominent. As we analyze data collected with a greater range of stimulus levels in more fibers, we will attempt to further characterize these effects.

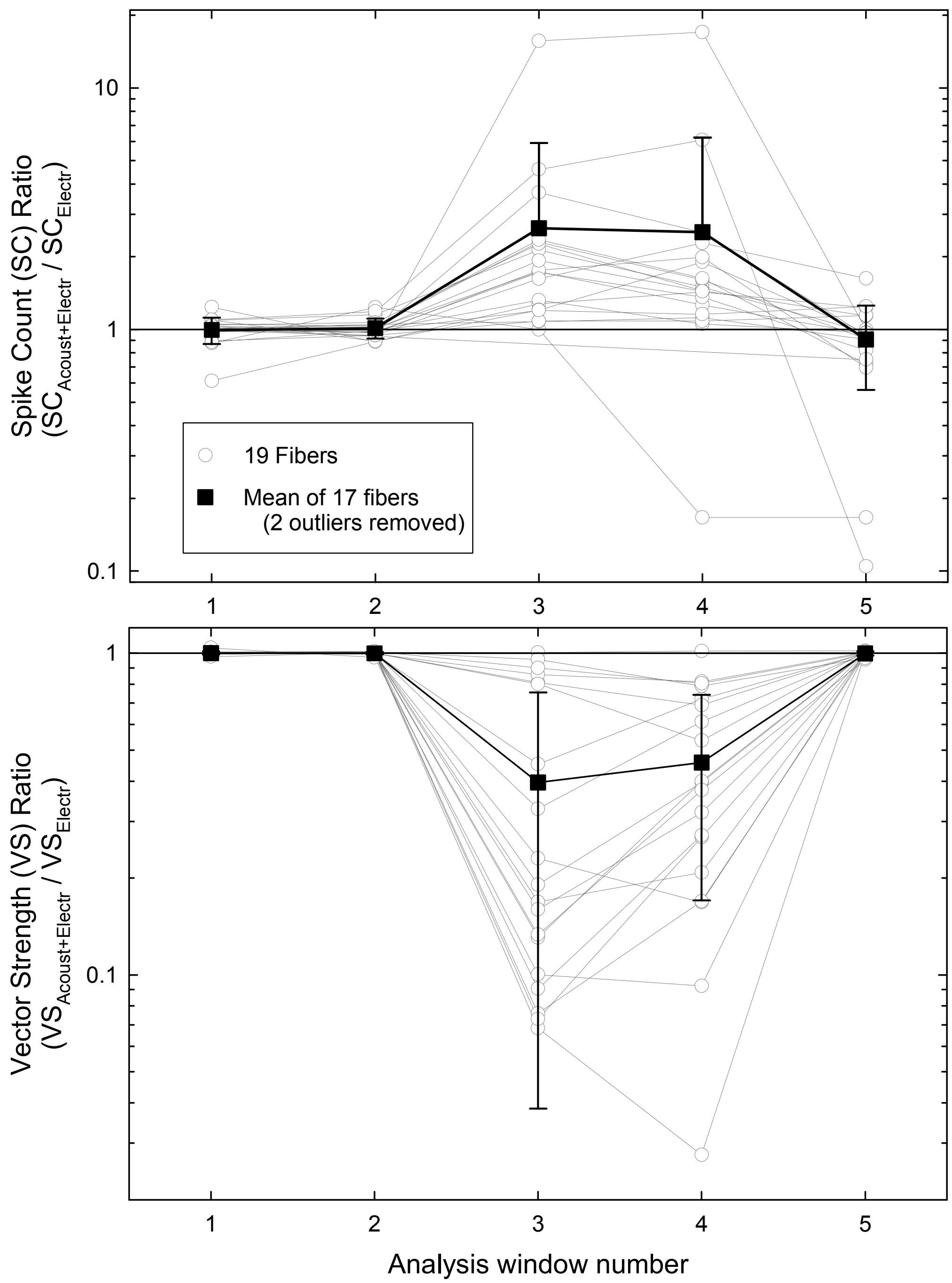


**Figure 6** Group data analysis for subject D10. Analyses of fiber responses (Spike count within a 20 ms window; Vector strength of responses within a 20 ms window) were carried out over five analysis windows as described in the text. Both spike count and vector strength are plotted as a function of analysis window number. Data from 19 fibers are plotted, along with mean values and standard deviations. In computing these two statistics, the uppermost and lowermost outliers (shown) were first removed In each case the acoustic noise level was 97 dB OAL and the electric level was chosen to be within 20 to 80% of the dynamic range (as assessed by firing efficiency to the first pulse).

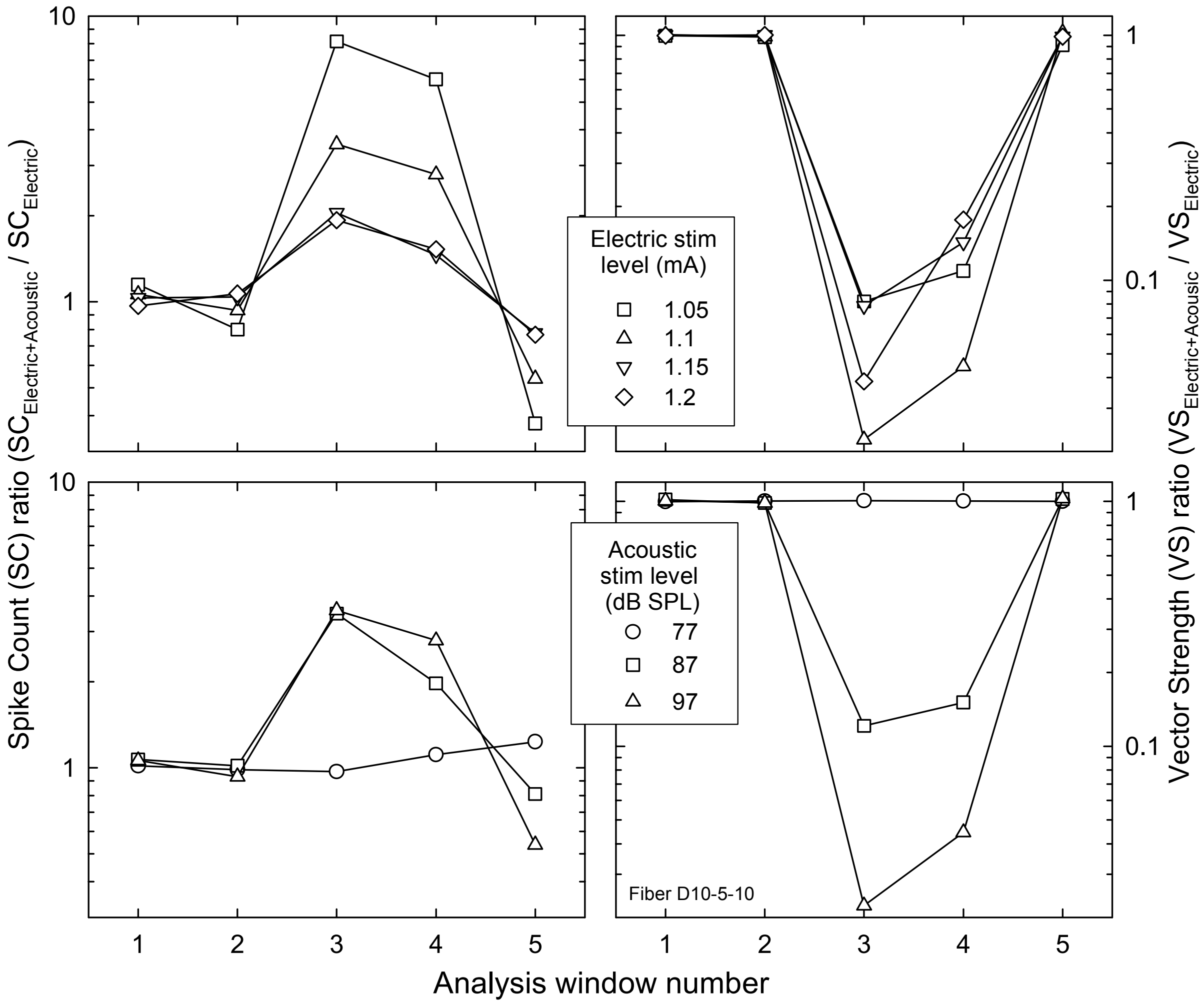


**Figure 7** Analyses of fiber D10-5-10 data using the same procedures as those used in Figure 6. In this case, data are plotted for a fiber where both the level of the electric stimulus (upper graphs) and the acoustic stimulus (lower graphs) were varied. Acoustic level in the upper graphs was fixed at 97 dB SPL. Electric level in the lower graphs was fixed at 1.15 mA.

### 4.4. Subsequent experiments

After our initial analysis of the data of subject D10, we have modified our procedures for data collection in several ways to better explore and quantify observed effects. First, we expanded the stimulus paradigm to include a "noise only" condition. In this way, we will collect data for every noise level used so as to better assess each fiber's acoustic range. Second, we have begun to incorporate an assessment of each fiber's best frequency in order to determine an across-cochlea spatial distribution of recorded fibers. This will be done as fiber contact-time permits. Finally, as our initial ECAP data were collected using longer duration pulse trains and noise bursts, we have begun using 400 ms pulse trains with 200 ms noise bursts (presented in the interval from 50 to 250 ms).

We are currently analyzing the data from these more recent experiments. One difference that is evident at this point is the presence of a more distinct residual effect on responses after noise offset. We speculate that this may be due to the longer duration of acoustic noise stimulation used in the later experiments. An example of a case where the residual effect of noise is very clear using longer-duration stimuli is shown in Figure 8. In this case, we show three histograms to our three stimulus conditions (acoustic alone, electric alone, and acoustic+electric). The comparison of the lower two graphs in the interval from 250 to 350 ms shows a marked decrease in response after noise offset.

### 4.5. Discussion

The initial results of single fiber responses to noise and pulse trains presented here are generally consistent with the interpretation of the ECAP data presented in the previous QPR. The noise affects the synchrony of the responses to pulse trains and consequently one would expect decreased amplitude of the ECAP. The time course of the effects of the noise is not yet clear however. There is an increase in discharge rate of single fibers at noise onset and a decline to a steady state response, typically at a higher rate than for the pulse train alone. The synchrony measures sometime show an onset effect but generally the effect on synchrony tends to be relatively constant. In contrast, the ECAP is observed to recover over the noise interval. In addition, the ECAP generally showed a decrease in amplitude after noise offset.

Initial data with single fibers has not shown as clear of a decrease in synchrony or discharge rate, but as we examine level effects in more detail (as in Figure 7) and investigate longer noise duration (as in Figure 8), we hope to provide a more complete model of the underlying single-fiber responses.

Proper understanding of the ECAP response patterns in terms of underlying single-fiber responses will require descriptions of the fiber population response, which would entail the examination of stimulus level effects and the assessment of fibers with a diversity of thresholds and cochlear sites of origin. In our future work, we hope to address some of these issues by examining, when feasible, stimulus level effects and determining the characteristic frequency of the fibers under study.

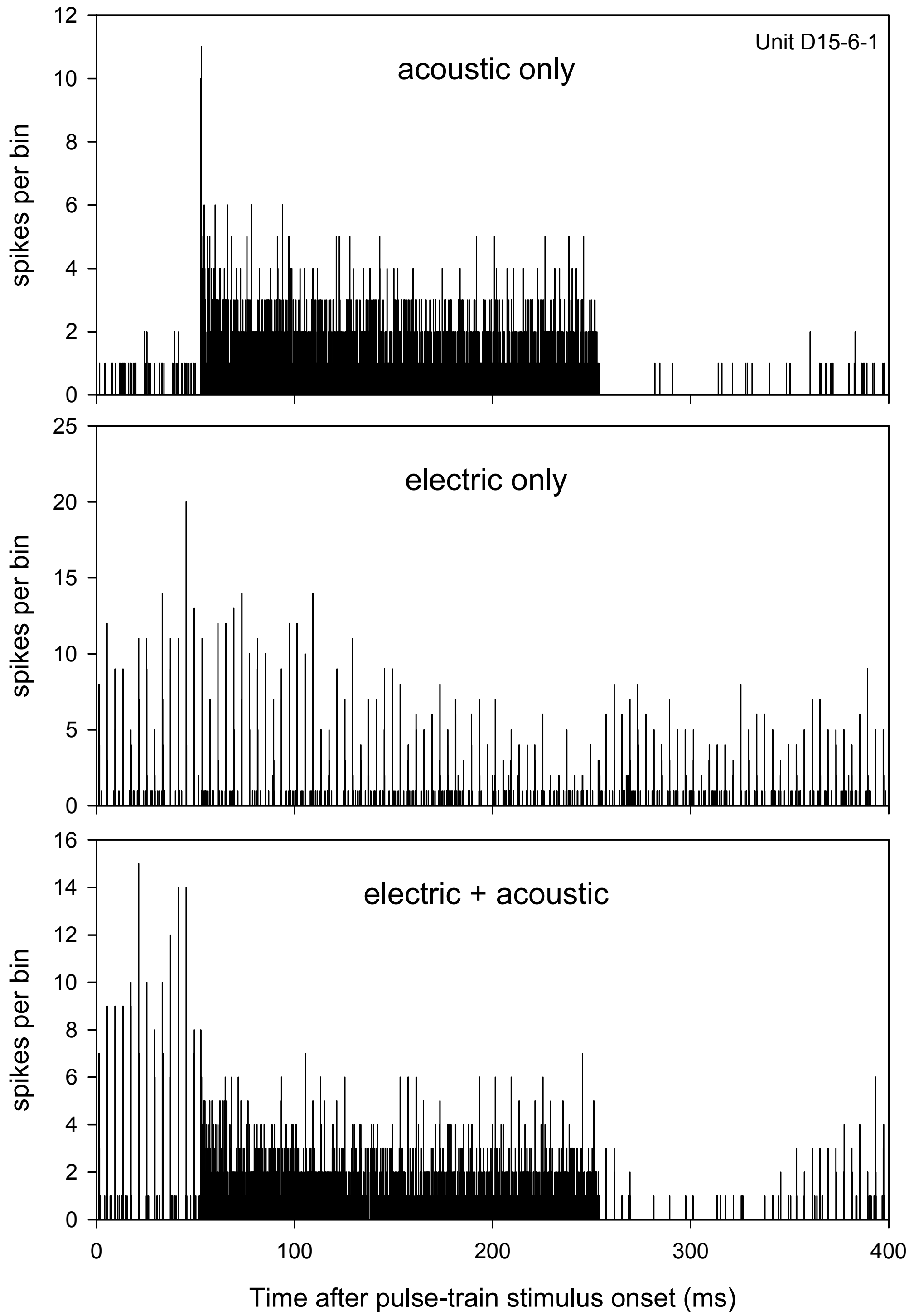


**Figure 8** Histograms in response to pulse trains 250-ms in duration with noise stimulus gated on at 50 ms and off at 250 ms. In this fiber, three stimuli were interleaved: (1) noise alone, (2) electric pulse train alone, and (3) combined acoustic and electric stimulation. The response to the pulse train after noise offset demonstrates a clear effect of the noise on the subsequent response to the electric pulse train.

## 5. Acoustic calibration

Acoustic calibration of levels presented to the feline ear canal was accomplished using a Radio Shack ¼ inch condenser microphone via a probe tube inserted into the speculum. The open end of the probe tube terminates within 0.5 mm of the speculum opening and the speculum is mated to the inside surface (lumen) of the canal near the cartilaginous/bony margin of the canal. Silk suture is used to compress the cartilage around the speculum in order to provide a good seal. The indwelling probe-tube assembly provides for the monitoring of sound pressure in the canal near the tympanic membrane during the course of the experiments.

Correction factors to account for the response of the probe tube and microphone assembly were determined using a symmetric, two-microphone, calibration cavity that provides for a comparison of an "unknown" microphone against a calibrated microphone. The probe tube was placed at one port of the cavity and a Larson-Davis ½ condenser microphone (Model 2559) was placed on the opposite port. Output of the latter microphone was measured on a matched Larson-Davis sound level meter. By delivering pure tones through third acoustic point (situated midway between the microphone ports), a function relating the probe microphone output voltage to sound pressure level was determined across frequencies. This correction function was then used in subsequent measures in animal preparations.

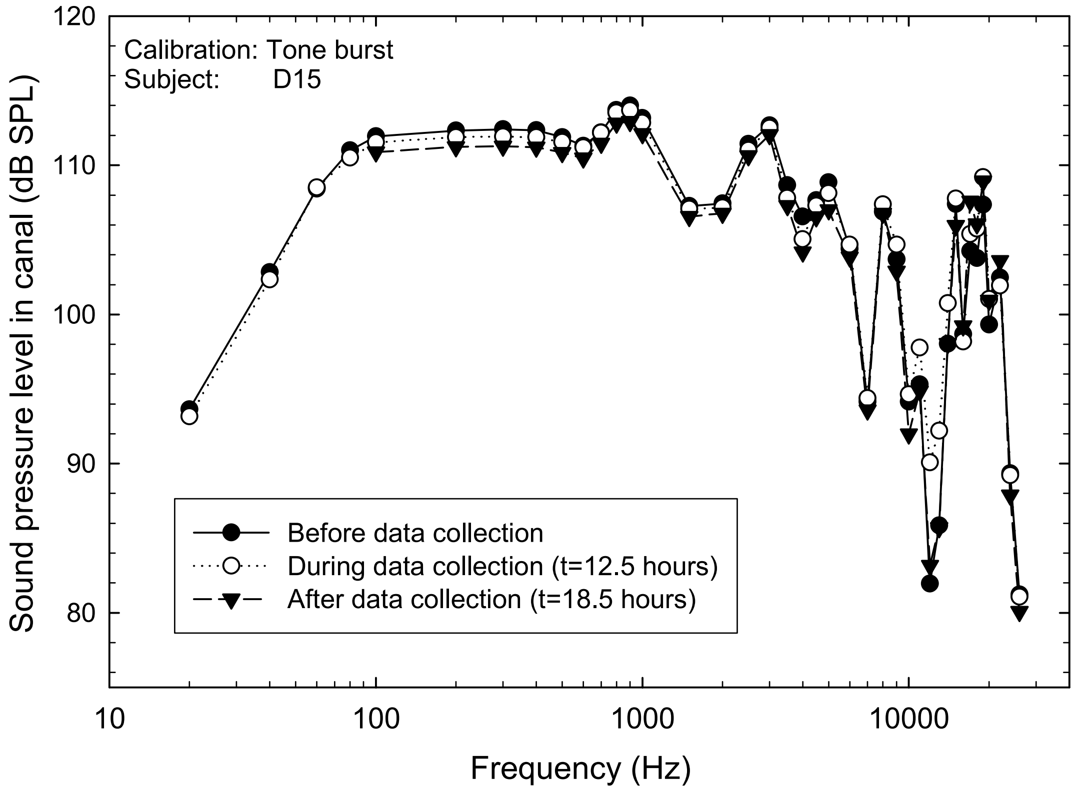


**Figure 9** Sound pressure levels corrected for the probe-tube-microphone calibration performed during the experimental session for subject D15. Shown are three sets of repeated measures obtained at different times during the course of the experimental session.

In each experiment, a Beyer DT-48 earphone was coupled to the excised ear canal via a speculum with the attached probe tube. To calibrate for each experiment, we generated tonal stimuli and recorded the probe microphone output using our Instrutech ITC-18 interface with Labview software. The voltage levels out are then corrected to produce a response frequency response at a fixed attenuation level for the closed acoustic system. Examples of the calibration curves measured in subject D15 are shown in Figure 9. In this case, calibration measures were performed three times during the 18-hour period of data collection period. The calibration values changed little over that period.

Our calibration routine also entails measurement of the response to the noise stimulus used for our wide-band acoustic noise stimulation. The noise stimulus is measured through the probe tube and therefore is affected by the probe calibration. Consequently, to assess overall level, we first measure the response in a band centered at 1kHz and calculate pressure spectrum level at that frequency. Overall sound pressure level (dB SPL OAL) is then determined using the corrected using the frequency calibration data such as that shown in Figure 9.

## 6. Plans for the next quarter

In the next quarter, we plan to do the following:

1. Perform additional analysis of the results presented in this report as well as analyze data from additional subjects with longer duration stimuli using the modified stimulus paradigm discussed in Section 4.3. Based on that analysis we will adjust parameters and/or methods to better assess patterns of interactions in future animal experiments.

2. We will analyze data from ongoing experiments using acute guinea pig preparations to study interaction of acoustic and electric stimuli with ECAP examining long-term effects.

3. Attend the Conference on Implantable Auditory Prostheses and present findings related to the research conducted under this contract.

# 7. References


1. **Hu, N., Abbas, P.J., Miller, C.A., Robinson, B.K., Nourski, K.V., Jeng, F.C., Abkes, B.A., Nichols, J.M. (2003).** Auditory response to intracochlear electric stimuli following furosemide treatment. (manuscript submittted to *Hear. Res*).

2. **Miller, C.A., Abbas, P.J., Robinson, B. K., Rubinstein, J. T., Matsuoka, A. J. (1999)** Electrically evoked single-fiber action potentials from cat: responses to monopolar, monophasic stimulation. Hear. Res. 130, 197-218.

3. **Miller, C.A., Abbas, P.J., Robinson, B.K. (2001).** Response properties of the refractory auditory nerve fiber. J Assoc Res Otolaryngol 2, 216-32.

4. **Miller, C.A., Abbas, P.J., Hu, N., Robinson, B.K. (2003).** Effects of remaining hair cells on cochlear implant function, *Second Quarterly Progress Report, Neural Prosthesis Program contract N01-DC-2-1005 NIH.*

5. **Sachs, M.B., Abbas, P.J. (1974)**. Rate versus level functions for auditory-nerve fibers in cats: tone-burst stimuli. J Acoust Soc Am 56, 1835-47.

5. **Verveen, A.A. (1961)** Fluctuation in Excitability, Drukkerij, Holland N.V., Amsterdam.